JACC Vol. 18, No. 3
September 1991:817–23

Nuclear Magnetic Resonance Imaging of the Palliative Operation for Hypoplastic Left Heart Syndrome

CHISATO KONDO, MD, CHRISTIAN HARDY, MD, FACC, SARAH S. HIGGINS, RN, J. NILAS YOUNG, MD, FACC, CHARLES B. HIGGINS, MD, FACC

San Francisco and Oakland, California

Electrocardiographic-gated nuclear magnetic resonance (NMR) imaging has been shown to be effective for the evaluation of congenital heart disease, particularly in supracardiac regions. This study evaluated the postoperative status after a stage I palliative operation (Norwood procedure) for hypoplastic left heart syndrome. The NMR images from three patients were compared with those of angiography and depicted all components of the reconstructed supracardiac and intracardiac anatomy after this operation. Nonobstructive anastomosis of the main pulmonary artery to the proximal aorta was clearly demonstrated in each patient. The caliber of the central or branch pulmonary artery, patency and caliber of the systemic to pulmonary artery shunt and the size of the atrial communication were also depicted in each patient and these findings corresponded with angiographic results.

The results suggest that NMR imaging is effective for assessing the results of initial palliative surgery for hypoplastic left heart syndrome, which seems to be important for managing patients before subsequent definitive surgery.

(J Am Coll Cardiol 1991;18:817–23)

Surgical management of hypoplastic left heart syndrome has steadily improved since the introduction of two-stage reconstructive surgery consisting of an initial palliative operation (Norwood procedure) and a subsequent modified Fontan operation (1,2). The aims of the initial palliative procedure include 1) anastomosis of the main pulmonary artery to the proximal aorta, thereby establishing permanent unobstructive blood flow from the right ventricle to the systemic arterial circulation; 2) establishment of pulmonary blood flow by a systemic to pulmonary artery shunt to promote normal growth and development of the pulmonary arteries; and 3) relief of pulmonary venous congestion by the creation of a nonrestrictive atrial septal defect (3).

After the initial palliative operation, it is necessary to assess important features of the reconstructed supracardiac anatomy, such as presence or absence of aortic arch obstruction, anatomy of the pulmonary artery, patency of the systemic to pulmonary shunt, status of the interatrial communication and right ventricular contractile and tricuspid valve function (4). The echocardiographic appearance after the initial palliative procedure has been previously described (5) and two-dimensional and Doppler echocardiography have been utilized to monitor the status of these patients. Nuclear magnetic resonance (NMR) imaging has advantages for evaluation of great vessel pathoanatomy because of the freedom of acoustic window limitations. Several reports (6–14) have demonstrated the capability of NMR imaging in the postoperative assessment of surgical procedures in the supracardiac region in patients with congenital heart disease. The effectiveness of NMR imaging for evaluating the postoperative status of the hypoplastic left heart syndrome has not been reported previously. Because of the tomographic thickness of NMR images during the early experience, these images were considered to be limited in the assessment of the cardiovascular anatomy in infants. Recent technical improvements have permitted the acquisition of an electrocardiographic (ECG)-gated thoracic image with thin slices (3 mm).

This report describes the appearance of the hypoplastic left heart syndrome after the initial palliative procedure. It indicates that the complex anatomy of this procedure can be depicted in infants with use of thin section multiplane images.

Methods

Study patients (Table 1). Three infants were studied 5 to 7 months after a palliative operation for hypoplastic left heart syndrome. Their age at the time of the nuclear magnetic resonance (NMR) study was 5, 7 and 17 months, respectively. These patients had visceroatrial situs solitus, d-ventricular loop and normally related great arteries. A hypoplastic left ventricle and obstructive lesions of the mitral or aortic valve, or both, were found in each patient.

The Norwood palliative operation in these patients consisted of atrial septectomy, division and patch closure of the distal main pulmonary artery and end to side anastomosis of

From the Department of Radiology, University of California, San Francisco and the Department of Pediatric Cardiology, Oakland Children's Hospital, Oakland, California.

Manuscript received June 19, 1990; revised manuscript received February 14, 1991, accepted March 19, 1991.

Address for reprints: Charles B. Higgins, MD, Department of Radiology, University of California, San Francisco, California 94143.

0735-1097/91/$3.50

JACC Vol. 18, No. 3
September 1991:817–23

Table 1. Clinical Characteristics of Three Patients

Pt No.	Age at Op (days)	Interval From Op to NMR Imaging (mo)	Anatomy	Systemic to Pulmonary Shunt
1	1	17	AS, MS, PDA, PFO	R M BT, L M BT
2	19	5	AA, MA, PDA, PFO	R BT
3	9	7	AS, MS, PDA, PFO	R M BT

AA = aortic atresia; AS = aortic stenosis; BT = Blalock-Taussig shunt; L = left; M = modified; MA = mitral atresia; MS = mitral stenosis; NMR = nuclear magnetic resonance; Op = operation; PDA = patent ductus arteriosus; PFO = patent foramen ovale; Pt = patient; R = right.

the pulmonary artery to the distal ascending aorta with incision and enlargement of the aortic arch, isthmus and ascending aorta with an aortic gusset (1). Systemic to pulmonary artery flow was reestablished through a graft between one or both subclavian arteries and the ipsilateral pulmonary artery (Table 1). The ages at operation ranged from 1 to 19 days.

Imaging methods. The infants were sedated with oral chloral hydrate (100 mg/kg body weight) 30 to 45 min before the NMR examination. Images were obtained with use of a 1.5 tesla superconducting magnet (General Electric). The ECG-gated, multislice spin-echo sequences were used with an echo delay time (TE) of 20 ms. The repetition time (TR) equaled the RR interval and thus depended on the patient's heart rate. The standard head coil was used for transmission and reception of radiofrequency pulses. The field of view was 320 to 240 mm. The acquisition matrix was 256 × 192 pixels interpolated to 256 × 256 pixels for display.

An initial multislice series in the sagittal plane was used to localize the diaphragm and superior border of the aortic arch. Subsequent images were acquired in the transverse plane (5-mm thick) and the data from two acquisitions were averaged. Additional images in the transverse plane (3-mm thick, separated by 0.5 mm) were obtained at the level of the pulmonary arteries and aortic arch. The 3-mm sections employed averaging of four acquisitions. Images in the sagittal plane (3-mm thick) through the aorta and pulmonary artery were also obtained.

One patient had an additional cine NMR sequence obtained by using gradient-echo imaging with a TE of 5 ms and a TR of 20 ms. Transverse images (5-mm thick) were obtained at the level of the anastomosis between the main pulmonary artery and the ascending aorta.

Conventional contrast angiography was performed for all patients and the results were compared with the NMR findings. The time interval between NMR imaging and angiography was 1 day, 6 days and 5 months, respectively. Findings from both studies were evaluated by different observers without knowledge of other data.

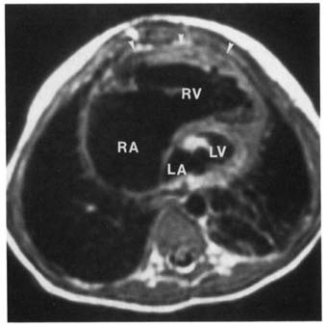

Figure 1. Patient 1. Transverse image showing a markedly enlarged right atrium (RA) and right ventricle (RV). Both the left atrium (LA) and the left ventricle (LV) were small. Right ventricular hypertrophy was also observed (arrowheads).

Results

Ventricle and atrium. A markedly enlarged right atrium and right ventricle and right ventricular hypertrophy were observed in all patients (Fig. 1). In contrast, the left atrial and left ventricular chambers were severely hypoplastic. A bright signal caused by stagnant flow was observed in the left ventricular chamber. These findings are characteristic of the hypoplastic left heart syndrome. The anatomy of the mitral valve and subvalve tensor apparatus was not clearly defined on nuclear magnetic resonance (NMR) images.

Aorta. The diminutive ascending aorta was shown on NMR images in all patients. At the origin of the aorta, coronary arteries were identified in every patient. The proximal aorta at the anastomosis between the proximal pulmonary artery and aortic arch was clearly depicted in each patient (Fig. 2). At the equivalent location to the spin-echo images, cine NMR images demonstrated blood flowing across the proximal anastomosis of the pulmonary artery to the ascending aorta as a bright signal (Fig. 2D). Stenosis at this anastomotic site was excluded in each patient. The distal aortic arch at the site of the juxtaductal suture line between the aortic arch gusset and the aortic arch was demonstrated in each patient (Fig. 3). The entire anatomy of the neo-aorta (that is, the reconstructed aorta) could be depicted on a single sagittal image (Fig. 4). Stenosis in the aortic arch was excluded in every patient.

Pulmonary artery. The anatomy of the central pulmonary arteries was depicted in every patient. Various degrees of narrowing of the central pulmonary arteries were shown on transverse images in all patients. In Patient 1, moderate narrowing of a long segment of the proximal left pulmonary artery and focal stenosis of the proximal right pulmonary

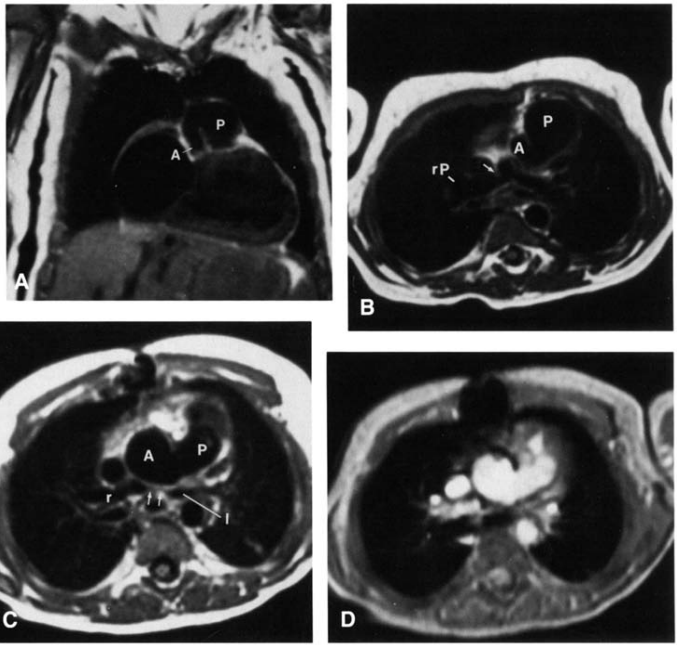

artery were observed (Fig. 5A). In Patient 2, segmental narrowing of the proximal left pulmonary artery was observed behind the aortic gusset (Fig. 5B). Localized stenosis was also shown at the proximal right pulmonary artery in this patient (Fig. 2B). However, there was a wide caliber of the distal left and right pulmonary arteries in Patients 1 and 2. In Patient 3, severe segmental narrowing or obstruction was observed at the proximal left pulmonary artery behind the aortic gusset (Fig. 5C). However, in this patient, differentiation between severe stenosis and obstruction was not clear on the spin-echo images. Cine NMR images demonstrated flowing blood as a bright signal in the distal left pulmonary artery in the same patient, excluding complete obstruction (Fig. 5D).

Atrial communication. A wide interatrial communication created by surgical resection of a part of the atrial septum was shown in each patient (Fig. 6). The connection of each pulmonary vein to the left atrium was also demonstrated.

Figure 2. Nuclear magnetic resonance (NMR) images demonstrating the pulmonary artery-ascending aorta anastomosis in two infants. **A,** Patient 2. Coronal image transecting the anastomosis of the ascending aorta (A) and the main pulmonary artery (P). The hypoplastic ascending aorta is shown (**arrow**). **B,** Patient 2. Transverse image showing that the anastomosis was widely opened, with no ridges producing obstruction. This image also depicts focal stenosis at the right pulmonary artery (rP) (**arrow**). **C,** Patient 3. Transverse spin-echo image showing nonobstructive anastomosis of the main pulmonary artery (P) and ascending aorta (A). This image also depicts severe narrowing or obstruction (**arrows**) between the right (r) and the left (l) pulmonary artery. **D,** Patient 3. Cine NMR image at an equivalent slice level to the spin-echo image demonstrates flowing blood across the anastomosis as a bright signal.

Shunt. All systemic to pulmonary artery shunts were demonstrated to be patent on NMR images (Fig. 3). The caliber of the shunt was narrow at the distal end of the graft in all patients.

JACC Vol. 18, No. 3
September 1991:817–23

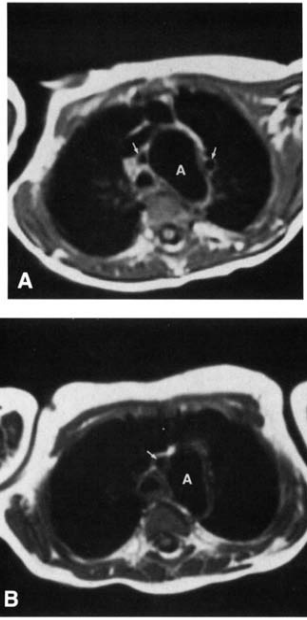

Figure 3. Nuclear magnetic resonance images demonstrating the caliber of the reconstructed aortic arch and status of the subclavian-pulmonary artery graft in two patients. **A**, Patient 1. Transverse image at the aortic arch (A) shows normal caliber at the distal aortic arch. Right and left modified Blalock-Taussig shunts were patent (**arrows**). **B**, Patient 2. Transverse image at the aortic arch (A). Distal anastomosis of an aortic gusset and aortic arch does not show any ridge protruding into the lumen; the caliber of the arch is normal. A patent right Blalock-Taussig shunt is shown as a circular structure with a central signal void (**arrow**).

Comparison between NMR and angiographic findings (Table 2). The results of NMR imaging agreed well with the angiographic results. Obstruction of the neo-aorta was excluded by both studies. The presence and location of narrowing of the central pulmonary artery and a systemic to pulmonary artery shunt documented by NMR imaging corresponded to the angiographic findings.

Discussion

The results of the current study show that nuclear magnetic resonance (NMR) imaging can provide morphologic assessment of each of the important components of the palliative Norwood operation used for the hypoplastic left heart syndrome. The anatomy of the neo-aorta and the pulmonary artery, the patency of the surgical shunts and the size of the interatrial communication demonstrated by NMR imaging were equivalent to those shown by angiography.

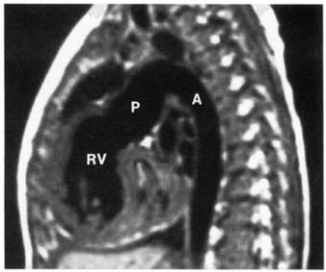

Figure 4. Patient 1. Sagittal image depicts the entire anatomy of a reconstructed aorta. No obstruction was found in the route from the right ventricle (RV) to the descending aorta (A). P = main pulmonary artery. Other abbreviations as in Figures 1 and 2.

Aortic arch obstruction after the Norwood procedure. The incidence of aortic arch obstruction has been reported (15) to be low after the first stage of the Norwood procedure. However, when it develops, recognition of it is critical because the concurrent increase in right ventricular pressure, along with the volume load imposed on the right ventricle, results in rapid deterioration of right ventricular function (4). Obstruction of the aortic arch can occur at any site on the arch. Proximal aortic obstruction can take the form of a lateral ridge projecting into the lumen at the suture line between the proximal pulmonary artery and the aortic arch gusset (5). Distal aortic arch obstruction can result from an anterolateral ridge at the distal suture line in the transverse arch or at the posterior juxtaductal region (5,15). Obstruction of the native proximal ascending aorta at the site of anastomosis with the pulmonary artery is also a theoretic complication; if it occurs, it will rapidly lead to myocardial ischemia or infarction due to coronary insufficiency. The current results demonstrated that adjacent multiple NMR images could document such anatomic changes of the lumen at any site of the aortic arch. Because NMR imaging can demonstrate anatomy from any desired direction by using transverse, coronal, sagittal and oblique planes, ridges at various position in the vascular lumen can be depicted from multiple imaging directions. In contrast, the demonstration of ridges at various locations in the aortic arch by conventional angiography may require complex angled projections and multiple injections of contrast media.

Pulmonary artery stenosis. In the current study, various degrees of stenosis of the central pulmonary arteries were

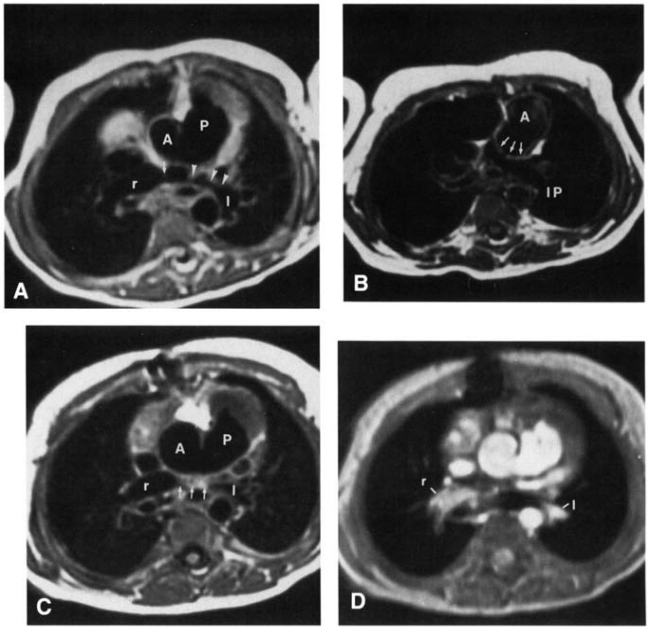

Figure 5 (above). Nuclear magnetic resonance (NMR) images displaying the caliber of the central pulmonary artery (P) in three patients. **A,** Patient 1. Transverse image showing segmental narrowing of the left (l) pulmonary artery (**arrowheads**). At the origin of the right (r) pulmonary artery, focal stenosis is also observed (**arrow**). A = aorta. **B,** Patient 2. Transverse image shows mild segmental narrowing at the origin of the left pulmonary artery (IP) behind the aortic (A) gusset (**arrows**). **C,** Patient 3. Transverse image showing severe narrowing or obstruction at the junction (**arrows**) between the right (r) and left (l) pulmonary arteries. A = aorta; P = main pulmonary artery. **D,** Cine NMR transverse images just caudal to **C** showing flowing blood in the right (r) and left (l) pulmonary arteries as a bright signal.

Figure 6 (below). Patient 1. Transverse image depicting wide interatrial communication. A lower pulmonary vein draining to the left atrium (LA) is also shown (**arrowheads**). RA = right atrium.

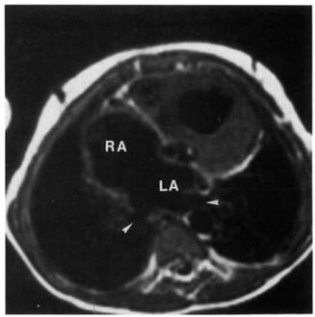

documented on NMR images. The capability of NMR imaging to depict the anatomy of the central pulmonary artery is important in evaluating candidates for a Fontan operation; suitability for this operation is critically dependent on near normal growth and development of the branch pulmonary arteries both centrally and peripherally (16,17). Although discrete proximal pulmonary stenosis can be relieved by

Table 2. Nuclear Magnetic Resonance Imaging and Angiographic Findings in Three Patients

Pt No.	NMR Imaging				Angiography			
	Neo-Aorta	Central PA	ASD	Shunt	Neo-Aorta	Central PA	ASD	Shunt
1	N/O	L seg (mod S) R focal (mild S)	N/O	R (S at J)	N/O	L (mod S) R (mod S)	N/O	R (S at J) L (N/O)
2	N/O	L seg (mod S) R focal (mild S)	N/O	R (S at J)	N/O	R (mild S)	N/O	R (S at J)
3	N/O	L seg (sev S)	N/O	R (S at J)	N/O	L (sev S [2.7 mm])	N/O	R (S at J)

ASD = atrial septal defect; J = junction with the pulmonary artery; mod = moderate; Neo-Aorta = reconstructed aorta; N/O = no obstruction; PA = pulmonary artery; S = stenosis; seg = segmental; sev = severe; other abbreviations as in Table 1.

angioplasty at operation, diffuse hypoplasia of a branch pulmonary artery may not be restored and may produce a poor outcome from a modified Fontan operation (18). After palliative surgery for hypoplastic left heart syndrome, relative hypoplasia of the left pulmonary artery has been noted in patients who have undergone a modified right Blalock-Taussig shunt; the cause has been suggested to be preferential flow to the right pulmonary artery from the right-sided shunt (19). These initial results suggest that NMR imaging is a reliable technique for excluding or documenting acquired hypoplasia of the pulmonary arteries (6,8–10). A previous report (6) has also shown that NMR imaging accurately defines the size of pulmonary arteries and the location and degree of stenosis of the central pulmonary arteries in patients with cyanotic congenital heart disease. Because the relation between the pulmonary artery and other anatomic structures such as the aortic gusset and main bronchus can be clearly depicted, the etiology of stenosis due to compression by these adjacent structures may be defined.

In the present study, stenoses of pulmonary arteries were usually found at the site of anastomosis with grafts or behind the aortic gusset. Eccentric vascular deformity in the anteroposterior direction caused by compression from the aortic gusset or patch may be difficult to depict on anteroposterior images with conventional contrast angiography. Coronal NMR imaging can provide images of the pulmonary arteries similar to those obtained with conventional contrast angiography and can depict eccentric vascular stenosis in the superoinferior direction (7). Finally, growth of distal pulmonary artery branches after a systemic to pulmonary artery shunt can be monitored sequentially by NMR imaging.

Systemic to pulmonary artery shunt patency. Rapidly progressive cyanosis after the palliative procedure is usually caused by limited blood flow through a systemic to pulmonary artery shunt (4). Rarely, cyanosis is due to pulmonary venous hypertension as a consequence of a restricted interatrial communication (15). NMR imaging can demonstrate the presence or absence of patency of a surgical shunt (20) and can depict the morphology, not only of the atrial septum but also of the orifices of the pulmonary veins in the left atrium (7,21). Therefore, NMR imaging should be able to define the cause of the progressive cyanosis and late pulmonary venous obstruction. In the present study, all patients were shown to have narrowing of the shunt at the distal end of the graft.

Evaluation of cardiac function and pulmonary blood flow. In addition to conventional spin-echo imaging, cine NMR imaging may be required for evaluation of cardiac function. Because this imaging sequence can attain high temporal resolution equivalent to that of contrast cineangiography, ventricular contractile function can be determined (22). Moreover, because flowing blood is demonstrated as a very bright signal on the images, the patency of surgical shunts can be identified (23). In the current study, cine NMR imaging was used in one patient (Patient 3) and showed blood flowing across the anastomosis between the pulmonary artery and the ascending aorta. The same patient was shown to have very severe narrowing at the proximal left pulmonary artery. Blood flow can be appreciated on cine NMR images and can thereby distinguish between severe stenosis and complete obstruction. In this patient, cine NMR imaging showed blood flow as a bright signal in the left pulmonary artery distal to the narrowing. Another technique for defining the presence of pulmonary blood flow is phase velocity mapping (24), which can differentiate flowing blood from stationary tissue and accurately quantitate flow velocity (25). Assessing tricuspid regurgitation and ventricular contractile function is important in evaluating the outcome after both the first-stage palliative surgery and the modified Fontan operation (26). Cine NMR imaging might be utilized in the future to evaluate the functional status of the tricuspid valve.

Conclusions. Nuclear magnetic resonance imaging is effective in assessing cardiovascular morphology of the initial palliative operation for hypoplastic left heart syndrome. Its ability to depict supracardiac anatomy permits the diagnosis of stenosis of the neo-aorta and central pulmonary arteries.

References

1. Norwood WI, Kirklin JK, Sanders SP. Hypoplastic left heart syndrome: experience with palliative surgery. Am J Cardiol 1980;45:87–90.
2. Norwood WI, Lang P, Hansen D. Physiologic repair of aortic atresia-hypoplastic left heart syndrome. N Engl J Med 1983;308:23–6.
3. Lang P, Norwood WI. Hemodynamic assessment after palliative surgery for hypoplastic left heart syndrome. Circulation 1983;68:104–8.

4. Norwood WI. Hypoplastic left heart syndrome. Cardiol Clin 1989;7:377–85.
5. Wainberg PM, Chin AJ, Murphy JD, Pigott JD, Norwood WI. Postmortem echocardiography and tomographic anatomy of hypoplastic left heart syndrome after palliative surgery. Am J Cardiol 1986;58:1228–32.
6. Canter CE, Gutierrez FR, Mirowitz SA, Martin TC, Hartmann AF. Evaluation of pulmonary arterial morphology in cyanotic congenital heart disease by magnetic resonance imaging. Am Heart J 1989;118:347–54.
7. Jolstad PR, Ehman RL, Hagler DJ, Ilstrup DM. Extracardiac vasculature in candidates for Fontan surgery: MR imaging. Radiology 1989;173:503–6.
8. Formanek AG, Witcofski RL, D'Souza VJ, Link KM, Karstaedt N. MR imaging of the central pulmonary arterial tree in conotruncal malformation. AJR 1986;147:1127–31.
9. Rees RSO, Somerville J, Underwood SR, et al. Magnetic resonance imaging of the pulmonary arteries and their systemic connections in pulmonary atresia: comparison with angiographic and surgical findings. Br Heart J 1987;58:621–6.
10. Kersting-Sommerhoff BA, Sechtem UP, Higgins CB. Evaluation of pulmonary blood supply by nuclear magnetic resonance in patients with pulmonary atresia. J Am Coll Cardiol 1988;11:166–71.
11. Baker EJ, Ayton V, Smith MA, et al. Magnetic resonance imaging of coarctation of the aorta in infants: use of a high field strength. Br Heart J 1989;62:97–101.
12. Soulen RL, Kan J, Mithell S, White RI Jr. Evaluation of balloon angioplasty of coarctation restenosis by magnetic resonance imaging. Am J Cardiol 1987;60:343–5.
13. Kersting-Sommerhoff BA, Sechtem UP, Fisher MR, Higgins CB. MR imaging of congenital anomalies of the aortic arch. AJR 1987;149:9–13.
14. Kersting-Sommerhoff BA, Seelos KC, Hardy C, Kondo C, Higgins SS, Higgins CB. Evaluation of surgical procedures for cyanotic congenital heart disease by using MR imaging. AJR 1990;155:259–66.
15. Pigott JD, Murphy JD, Barber G, Norwood WI. Palliative reconstructive surgery for hypoplastic left heart syndrome. Ann Thorac Surg 1988;45:122–8.
16. Choussat A, Fontan F, Besse P, Vallot A, Chauve A, Bricaud H. Selection criteria for Fontan's procedure. In: Anderson RH, Schneeburne EA, eds. Paediatric Cardiology 1977. Edinburgh: Churchill Livingstone; 1977:567–80.
17. Nakata S, Imai Y, Takanashi Y, et al. A new method for the quantitative standardization of cross-sectional areas of the pulmonary arteries in congenital heart disease with decreased pulmonary blood flow. J Thorac Cardiovasc Surg 1984;88:610–9.
18. Norwood WI, Piggot JD, Murphy JD, Ranhaely RC. Modified Fontan reconstructive surgery for hypoplastic left heart syndrome (abstr). Circulation 1987;76(suppl III):III-73.
19. Alboliras ET, Chin AJ, Barber G, Helton JG, Piggot JD, Norwood WI. Pulmonary artery configuration after palliative operations for hypoplastic left heart syndrome. J Thorac Cardiovasc Surg 1989;97:878–85.
20. Jacobstein MD, Fletcher BD, Nelson AD, Ciampoli M, Alfidi RJ, Riemenschneider TA. Magnetic resonance imaging: evaluation of palliative systemic-pulmonary artery shunts. Circular on 1984;70:650–6.
21. Diethelm L, Dery R, Lipton M, Higgins CB. Atrial-level shunts: sensitivity and specificity of MR in diagnosis. Radiology 1987;162:181–6.
22. Sechtem U, Pflugfelder PW, White RD, et al. Cine MRI: potential for the evaluation of cardiovascular function. AJR 1987;148:239–46.
23. White RD, Pflugfelder PW, Liston MJ, Higgins CB. Coronary artery bypass grafts: evaluation with cine MR imaging. AJR 1988;150:1271–4.
24. Underwood SR, Firmin DN, Klipstein RJ, Rees RSO, Longmore DB. Magnetic resonance velocity mapping: clinical application of a new technique. Br Heart J 1987;57:404–12.
25. Kondo C, Caputo GR, Semelka R, Foster E, Shimakawa A, Higgins CB. Right and left ventricular stroke volume measurements with velocity encoded cine MR: in vivo and in vitro validation. AJR Am J Roentgenol 1991;157:9–16.
26. Barber G, Helton JG, Aglira BA, et al. The significance of tricuspid regurgitation in hypoplastic left-heart syndrome. Am Heart J 1988;116:1563–7.